Structure of Methanol Confined in MCM-41 Investigated by Large-Angle X-ray Scattering Technique

Toshiyuki Takamuku,*,† Hirokazu Maruyama,† Shigeharu Kittaka,‡ Shuichi Takahara,‡ and Toshio Yamaguchi§

Department of Chemistry and Applied Chemistry, Faculty of Science and Engineering, Saga University, Honjo-machi, Saga 840-8502, Japan, Department of Chemistry, Faculty of Science, Okayama University of Science, 1-1 Ridaicho, Okayama 700-0005, Japan, and Advanced Materials Institute and Department of Chemistry, Faculty of Science, Fukuoka University, Nanakuma, Jonan-ku, Fukuoka 814-0180, Japan

Received: June 17, 2004; In Final Form: October 9, 2004

Large-angle X-ray scattering (LAXS) measurements over a temperature range from 223 to 298 K have been made on methanol confined in mesoporous silica MCM-41 with two different pore diameters, 28 Å (C14) and 21 Å (C10), under both monolayer and capillary-condensed adsorption conditions. To compare the structure of methanol in the MCM-41 pores with that of bulk methanol, X-ray scattering intensities for bulk methanol in the same temperature range have also been measured. The radial distribution functions (RDFs) for the monolayer methanol samples showed that methanol molecules are strongly hydrogen bonded to the silanol groups on the MCM-41 surface, resulting in no significant change in the structure of adsorbed methanol with respect to the pore size and temperature. On the other hand, the RDFs for the capillary-condensed methanol samples showed that hydrogen-bonded chains of methanol molecules are formed in both pores. However, the distance and number of hydrogen bonds estimated from the RDFs suggested that hydrogen bonds between methanol molecules in the pores are significantly distorted or partly disrupted. It has been found that the hydrogen bonds are more distorted in the smaller pores of MCM-41. With decreasing temperature, however, the hydrogen-bonded chains of methanol in the pores were gradually ordered. A comparison of the present results on methanol in MCM-41 pores with those on water in the same pores revealed that the structural change with temperature is less significant for confined methanol than for confined water.

Introduction

Mesoporous materials, such as silica gel and zeolite, have been used in high-performance liquid chromatography (HPLC) and in the catalysis of chemical reactions. In biochemistry, water confined in pores has attracted much attention as a model of unfrozen water in biological cells and tissues because water in the pores can easily be kept supercooled in a temperature range down to ∼223 K. The microscopic behavior of liquids confined in pores is very important for understanding the properties, chemical equilibria, and catalyst reactions in the pores.

In the past 2 decades, X-ray and neutron scattering and ^{1}H NMR measurements have often been performed on water confined in mesoporous silica to elucidate its structure and dynamics at the molecular level.[1−10] Many investigations showed that, at ambient temperatures, the structure of water in the pores is not significantly different from that in bulk water. On the other hand, at undercooled conditions, cubic ice is often formed in the pores, not normal hexagonal ice. Thus, many authors proposed a confinement effect on the water structure in the pores that is similar to a pressure effect in the bulk. Smirnov et al. made large-angle X-ray scattering (LAXS) measurements over a temperature range of 223−298 K on water confined in the mesoporous MCM-41 materials C14 and C10 with highly controlled pore diameters.[11] They succeeded in clarifying the structures of water under monolayer and capillary-condensed conditions; in the monolayer, water molecules adsorbed on the surface water molecules are bound to the silanol groups with a short O···O hydrogen bond of ∼2.6 Å, while the tetrahedral-like structure of water is formed at the central part of the pores, though the structure is partly distorted. Moreover, they found that the water structure is gradually enhanced in the pores with decreasing temperature.

For organic solvents, which are often used for HPLC and so forth rather than water, physicochemical properties in mesoporous silicas have been investigated by using various techniques. Jonas and co-workers have clarified the dynamics of various organic solvents, such as pyridine, dioxane, and ethanol, confined in silca glasses with different pore diameters by using an NMR relaxation method.[12,13] They have estimated spin−lattice relaxation rates of the surface-layer organic solvents from observed spin−lattice relaxation rates in terms of a two-state, fast-exchange model, where two distinct phases, bulk and surface-affected, are assumed in the pores. It has been found that the reorientational motion of an organic solvent in the surface layer is more strongly restricted depending on its ability to hydrogen bond to a silica surface. Morishige and Kawano have investigated freezing and melting behaviors of methanol confined in MCM-41 and SBA-15 with different pore sizes by using an LAXS method.[14] On the basis of the X-ray diffraction patterns, they discussed a pore-size effect on vitrification, crystallization, and phase transition between α and β states of methanol in the pores. However, the structure of organic

* To whom all correspondence should be addressed. E-mail: takamut@cc.saga-u.ac.jp. Phone: +81-952-28-8554. Fax: +81-952-28-8548.
† Saga University.
‡ Okayama University of Science.
§ Fukuoka University.

10.1021/jp047359k CCC: $30.25 © 2005 American Chemical Society
Published on Web 12/03/2004

TABLE 1: Parameters of the Synthesized MCM-41 C14 and C10 Samples

	surface area ($m^2\ g^{-1}$)	pore diameter (Å)	pore volume ($cm^3\ g^{-1}$)
C14	1300	28	0.926
C10	1069	21	0.496

solvents, such as methanol, in the pores has still been ambiguous at the molecular level.

The previous LAXS[15] and large-angle neutron scattering (LANS) with H/D isotopic substitution[16] investigations on bulk methanol showed that methanol molecules form a mainly one-dimensional zigzag chain structure via hydrogen bonding,[15] in contrast to the three-dimensional tetrahedral-like network in bulk water.[15,17,18] Thus, it is very interesting to see how hydrogen bonding differs between methanol and water molecules when they are confined in pores.

In the present investigation, we have made LAXS measurements over a temperature range from 223 to 298 K on methanol adsorbed under both monolayer and capillary-condensed conditions in MCM-41 materials, C14 and C10, which are the same materials investigated by Smirnov et al.[11] MCM-41 materials were chosen to elucidate pore-size and temperature effects on liquid structure because they contain highly controlled cylindrical channels. For comparison, bulk methanol was also measured in the same temperature range of 223−298 K. On the basis of the present results, the structure of methanol confined in the MCM-41 pores is discussed along with the temperature and pore size. Structural differences between methanol and water in the pores are discussed at the molecular level.

Experimental Section

Preparation of MCM-41 Samples. Two kinds of mesoporous silica MCM-41, C14 and C10, were synthesized by the method of Beck et al.[19] using alkyltrimethylammonium bromide with alkyl chains of 14 and 10 C atoms, respectively. The frameworks of the synthesized MCM-41 materials were analyzed by transmission electron microscopy and powder X-ray diffraction. Regular hexagonally packed arrays and uniform pore channels of MCM-41 were clearly observed. The powder X-ray diffraction pattern showed three Bragg peaks of (100), (110), and (200), which is characteristic of MCM-41.[19] A N_2 adsorption analysis at liquid-N_2 temperature was made on the MCM-41 materials. To evaluate the surface area and the pore diameter of the MCM-41 materials, the corresponding values by the Brunauer−Emmett−Teller plot and the Dollimore and Heal method[20] are summarized in Table 1.

Methanol (Wako, grade for HPLC) was dried with thermally activated 4-Å molecular sieves for several days. To evaluate adsorption of methanol in the MCM-41 C14 and C10 pores, adsorption and desorption isotherms at 298 K were measured by weighing methanol adsorbed into the MCM-41 pores with an electronic balance (BEL, Rubotherm) connected to a vacuum line, where methanol vapor pressure can be controlled. Parts a and b of Figure 1 show adsorption and desorption isotherms of methanol on the MCM-41 C14 and C10, respectively, as a function of methanol vapor pressure. The figures show no hysteresis between adsorption and desorption isotherms for either MCM-41 C14 or C10. Furthermore, methanol is adsorbed in the MCM-41 pores in two steps; the first step, at lower methanol vapor pressures, arises from the formation of monolayer methanol on the pore surface, while the second one, at higher pressure, corresponds to the capillary condensation of

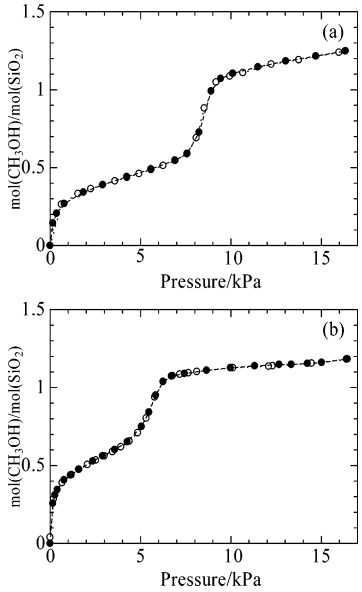

Figure 1. Adsorption isotherms of methanol on the MCM-41 C14 (a) and C10 (b) at 298 K. The symbols of filled and opened circles represent adsorption and desorption, respectively.

methanol at the central part of the pores. The sharp jump between the first and second steps suggests very narrow distribution of the pore diameters for the MCM-41 C14 and C10 synthesized.

LAXS Measurements. A soda-glass capillary (W. Müller Co.) of 2-mm inner diameter and 0.01-mm wall thickness was filled with MCM-41 material. The MCM-41 sample was dried under a vacuum at 353 K for 6 h. Then, the MCM-41 pores were filled with methanol by using an in situ adsorption apparatus with a vacuum line. Both drying and filling processes were repeated three times to remove water initially adsorbed on the pore surfaces. Finally, according to the adsorption isotherms (Figure 1), monolayer methanol samples were prepared by adsorbing methanol into the MCM-41 C14 and C10 pores at methanol vapor pressures of 5.0 and 4.0 kPa, respectively, for 6 h, while capillary-condensed methanol samples of C14 and C10 were prepared at vapor pressures of 12.0 and 10.0 kPa, respectively, for 12 h. After the adsorption of methanol, the open end of the capillary was sealed with epoxy glue to keep the sample under the same conditions during X-ray measurements.

X-ray scattering intensities from the above four MCM-41 samples were measured over the temperature range of 223−298 K with a rapid liquid X-ray diffractometer (Bruker AXS, DIP301) using an imaging plate (IP) as a two-dimensional area detector, which is described elsewhere.[21] X-rays were generated by a rotary Mo anode (Rigaku, RU-300) operated at 50 kV and 200 mA and then monochromatized with a flat graphite crystal to obtain Mo Kα radiation ($\lambda = 0.7107$ Å). A double-hole type collimator, whose hole diameter is 0.9 mm, was used. The exposure time was 1 h for each sample. The X-ray beam position was adjusted to irradiate the sample at a distance from the epoxy sealing to avoid contamination by volatile components from the epoxy glue. The observed range of the scattering angle (2θ) was 0.2−109°, corresponding to the scattering vector s ($=4\pi\lambda^{-1}\sin\theta$) of 0.03−14.4 $Å^{-1}$.

Cooling of the sample was carried out by using a specially designed cryostat that blew cold N_2 gas from liquid N_2 onto the capillary. The temperature of the sample was measured by a copper−constantan thermocouple and controlled within ±1 K by adjusting the blow rate of N_2 gas.

After the X-ray measurements for the MCM-41 sample with adsorbed methanol, the tip of the capillary was opened again by breaking it. Then, to prepare a dry MCM-41 sample, the adsorbed methanol was evaporated from the MCM-41 pores by connecting the sample to the vacuum line. The X-ray scattering intensities of the dry MCM-41 sample at 298 K were also measured as background.

X-ray scattering intensities of the MCM-41 sample with adsorbed methanol, $I_s(s)$, are expressed by

$$I_s(s) = I_{MeOH}(s) + I_{MeOH-MCM}(s) + I_{MCM}(s) + I_{gc}(s) \quad (1)$$

where $I_{MeOH}(s)$ represents X-ray scattering intensities from adsorbed methanol, $I_{MeOH-MCM}(s)$ represents intensities from interactions between adsorbed methanol and the MCM-41 surface, $I_{MCM}(s)$ represents those from MCM-41, and $I_{gc}(s)$ represents those from the glass capillary. All of the intensities were corrected for polarization and absorption.[21,22] On the other hand, X-ray scattering intensities of the dry MCM-41 sample, $I_{dry}(s)$, are expressed by

$$I_{dry}(s) = I_{MCM}(s) + I_{gc}(s) \quad (2)$$

Therefore, the X-ray scattering intensities related to the adsorbed methanol in the pores were obtained by subtracting eq 2 from eq 1 as

$$I_s(s) - I_{dry}(s) = I_{MeOH}(s) + I_{MeOH-MCM}(s) \quad (3)$$

The structure function, $i(s)$, is given by

$$i(s) = K[I_{MeOH}(s) + I_{MeOH-MCM}(s)] - \sum x_j f_j^2(s) \quad (4)$$

where K represents a factor to normalize the experimental intensities to absolute units in the usual manner,[23−25] x_j is the number of atom j in a stoichiometric volume, V, containing one O atom from a methanol molecule, and $f_j(s)$ is the atomic scattering factor of atom j corrected for the anomalous dispersion. The structure function was Fourier transformed into the radial distribution function (RDF) $D(r)$ by eq 5 in ref 11. To perform a quantitative analysis of the X-ray data, a comparison between the experimental structure function and the theoretical one, which was calculated on a structure model with eq 7 in ref 11, was made by a least-squares refinement procedure using eq 6 in ref 11.

To compare the structure of methanol adsorbed into the MCM-41 pores with that of bulk methanol, X-ray scattering measurements were also made on pure methanol over the temperature range of 223−298 K. Methanol was sealed into a soda-glass capillary (2-mm inner diameter). X-ray scattering intensities of the methanol sample were measured as described above, and those of an empty capillary were also done as background. Densities of methanol below 273 K were estimated by extrapolation of those measured by using a densimeter (Anton Paar KG, DMA60) in a temperature range from 283 to 308 K.

The present X-ray scattering data were treated by the programs KURVLR[26] and NLPLSQ.[27]

Results and Discussion

Total RDFs. The *s*-weighted structure functions $i(s)$ for bulk methanol and monolayer and capillary-condensed methanol in the MCM-41 C14 and C10 pores over the temperature range of 223−298 K are shown in Figures 2−4, respectively. The corresponding RDFs in the form of $D(r) - 4\pi r^2\rho_0$ are illustrated in Figures 5−7, respectively.

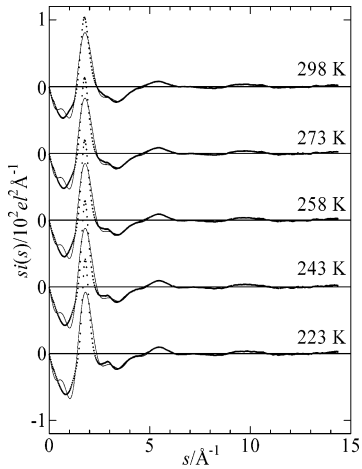

Figure 2. Structure functions $i(s)$ multiplied by s for bulk methanol at various temperatures. The dots and solid lines represent experimental and calculated values, respectively.

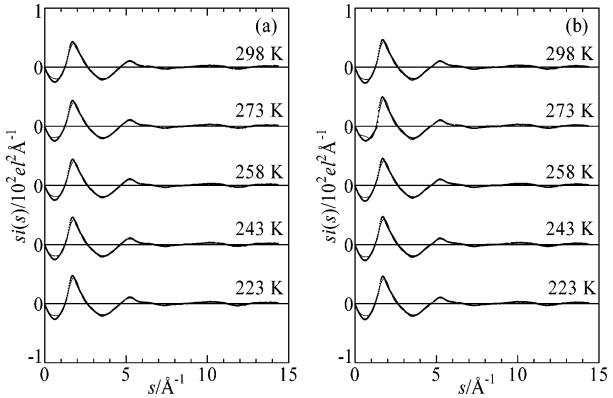

Figure 3. Structure functions $i(s)$ multiplied by s for the monolayer methanol in MCM-41 C14 (a) and C10 (b) at various temperatures. The dots and solid lines represent experimental and calculated values, respectively.

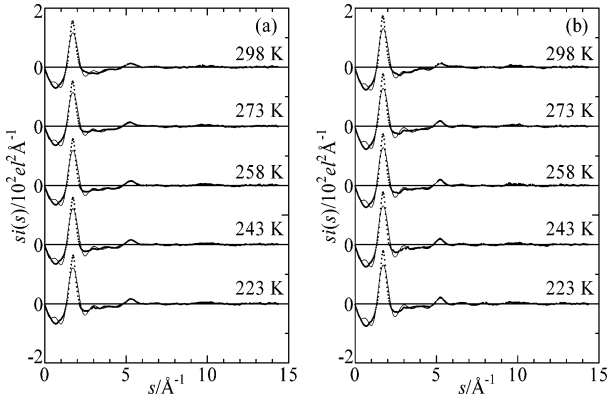

Figure 4. Structure functions $i(s)$ multiplied by s for the capillary-condensed methanol in MCM-41 C14 (a) and C10 (b) at various temperatures. The dots and solid lines represent experimental and calculated values, respectively.

Bulk Methanol. The structure of bulk methanol at 298 K has already been reported in refs 15 and 16 and, thus, is briefly described here. In the RDF (Figure 5), two peaks at 1.4 and 2.1 Å arise from intramolecular interactions within a methanol molecule; the 1.4-Å peak is from the C−O bond, and the small 2.1-Å one is from the nonbonding C···H(OH) and O···H(CH_3) interactions. A peak at 2.8 Å is assigned to O···O hydrogen bonds between methanol molecules. Large and broad multiple peaks in the r range of 3.5−5.5 Å are attributed to the first-

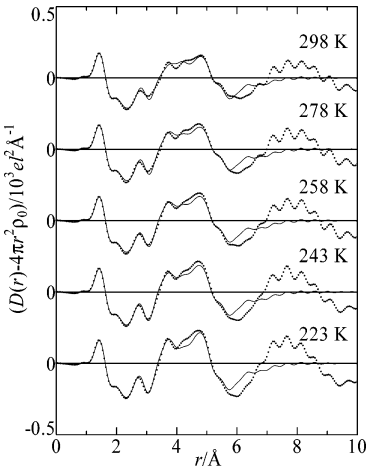

Figure 5. RDFs in the form of $D(r) - 4\pi r^2\rho_0$ for bulk methanol, which were obtained by Fourier transformation of the structure functions in Figure 2. The dots and solid lines represent experimental and calculated values, respectively.

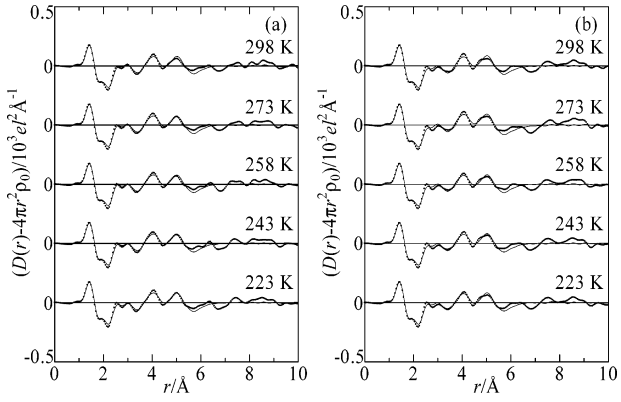

Figure 6. RDFs in the form of $D(r) - 4\pi r^2\rho_0$ for the monolayer methanol in MCM-41 C14 (a) and C10 (b), which were obtained by Fourier transformation of the structure functions in Figure 3. The dots and solid lines represent experimental and calculated values, respectively.

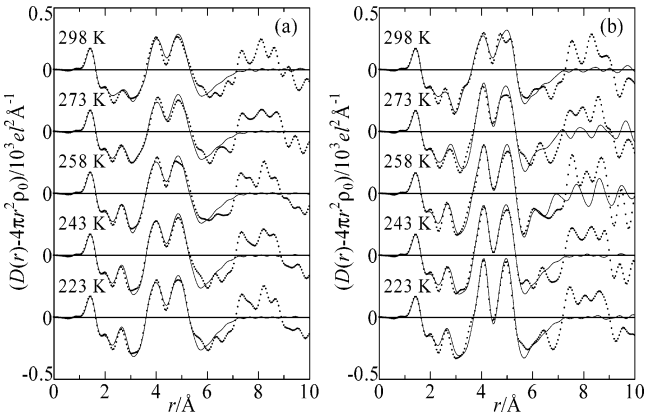

Figure 7. RDFs in the form of $D(r) - 4\pi r^2\rho_0$ for the capillary-condensed methanol in MCM-41 C14 (a) and C10 (b), which were obtained by Fourier transformation of the structure functions in Figure 4. The dots and solid lines represent experimental and calculated values, respectively.

and second-neighbor intermolecular interactions, such as C···C (∼3.7 Å), O···O (∼4.5 Å), andO···C (∼4.8 Å) interactions.[15] Other broad multiple peaks in the r range of 6.5−9.5 Å are assigned to the third- and fourth-neighbor interactions. These features reveal that four or five methanol molecules form a chain structure by hydrogen bonding in the bulk.

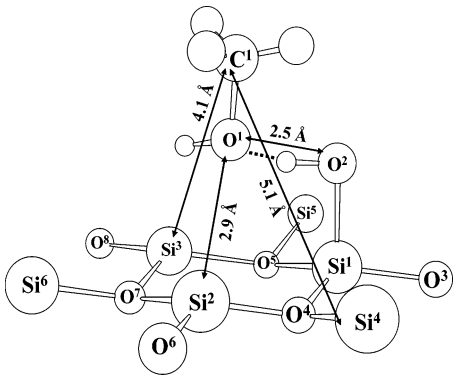

Figure 8. Possible model of monolayer methanol adsorbed on the MCM-41 surface. The dashed line represents a hydrogen bond between the methanol O atom and the H atom of the silanol group. For Si^2-Si^5 atoms, one O atom or one hydroxyl group in the tetrahedral SiO_2 structure is omitted for simplicity.

When the temperature decreases, the peaks at 2.8, 4.5, and 8 Å grow slightly. However, a drastic change in the RDFs with a change in temperature is not observed because even the lowest temperature investigated (223 K) is still higher than the freezing point (175 K) of methanol. This is in agreement with results from LANS with H/D isotope substitution measurements on liquid methanol;[16] the methyl−methyl pair correlation functions of g_{CC} obtained by an empirical potential structure refinement (EPSR) slightly change with decreasing temperature from 298 to 193 K. On the other hand, the hydroxyl−hydroxyl pair correlation functions of g_{OH} and g_{HH} are strongly affected by the temperature change. However, the average number of hydrogen bonds between methanol molecules and the average length of hydrogen-bonded methanol chains estimated from the pair correlation functions slightly change at both temperatures. It was thus suggested that the orientation between methanol molecules is strengthened along the O−H···O hydrogen bond when the temperature decreases from 298 to 193 K, but the hydrogen-bonded chains are not practically lengthened with a decrease in temperature.[16] Although the present X-ray experiments could not observe the correlations of H−H, H−C, and H−O pairs well because of the very small X-ray scattering power of the H atom, the change in the RDFs with decreasing temperature suggests the same structural change as that observed by the LANS measurements.

Monolayer Methanol. Figure 6a shows the RDFs for the monolayer methanol confined in the MCM-41 C14 pores at various temperatures. Except for the 1.4- and 2.1-Å peaks of the intramolecular interactions within a methanol molecule, the RDF for the monolayer methanol at 298 K is obviously different from that for bulk methanol; (1) the peak at 2.8 Å observed for bulk methanol, which is related to O···O hydrogen bonds between methanol molecules, is separated into two peaks at 2.5 and 2.9 Å, (2) the large and broad peak centered at 4.5 Å observed in the RDF for the bulk is weakened and split into two small peaks at 4.1 and 5.1 Å, and (3) the broad peak at 8.0 Å observed for the bulk almost disappears in the RDF for the monolayer methanol. These results indicate that the structure of methanol on the surface of the MCM-41 pores is significantly different from that of bulk methanol.

The above characteristics of the RDF for the monolayer methanol have led us to build a plausible structure model of methanol adsorbed on the surface, as depicted in Figure 8 with important interatomic distances. In this model, a methanol molecule is bound to the silanol group with a short O···O hydrogen-bonding distance of 2.5 Å and positioned over the

center of a six-membered ring of SiO_2. The distance of O···O hydrogen bonds between a methanol molecule and the silanol group is much shorter than that (2.77 Å) between methanol molecules in the bulk, as has been found in water in MCM-41 pores,[11] suggesting that a methanol molecule is strongly bound to the silanol group. As discussed for monolayer water in MCM-41 pores, the very short hydrogen bond between the methanol molecule and the silanol group may be caused by the acidic nature of the silanol group ($-Si-O^-H^+$). The 2.9-Å peak in the RDF may correspond to the O···$Si^{2,3}$ interaction between the hydroxyl O atom of a methanol molecule and the second-neighbor Si atom in the SiO_2 network. The peaks at 4.1 and 5.1 Å in the RDF may originate from nonbonding C^1···$Si^{2,3}$ and C^1···$Si^{4,5}$ interactions, respectively. The interaction between the hydroxyl O^1 atom of a methanol molecule and the Si^1 atom of the silanol group appears at 3.65 Å as a tail of the 4.1-Å peak.

When the temperature is lowered down to 223 K, these peaks do not change remarkably, suggesting again that methanol molecules are strongly bound to the silanol groups as well as to the monolayer water in MCM-41 pores.[11]

As seen in Figure 6b, the RDFs for the monolayer methanol in the smaller pores of the MCM-41 C10 at various temperatures are very similar to those in the MCM-41 C14 pores at the corresponding temperatures. It is thus concluded that the structure of methanol strongly hydrogen bonded to the surface is scarcely affected by the pore size.

Capillary-Condensed Methanol. Figure 7a shows the RDFs for the capillary-condensed methanol in the MCM-41 C14 pores at various temperatures. The RDF for the capillary-condensed methanol at 298 K shows features similar to those for bulk methanol; a peak at 2.6 Å and two large and broad multiple peaks in the *r* ranges of 3.5−5.5 and 6.5−9.5 Å are observed. The 2.6-Å peak is assigned to O···O hydrogen bonds between methanol molecules at the central part of the pores, although the short O···O hydrogen bonds between methanol molecules and the silanol groups on the surface also contribute to this peak, as discussed above. It is expected that the two large and broad multiple peaks at 3.5−5.5 and 6.5−9.5 Å are attributed to the first- and second-neighbor interactions in methanol chains and the third- and fourth-neighbor ones, respectively. Hence, these features suggest that methanol molecules form hydrogen-bonded chains even in the MCM-41 C14 pores of 28-Å diameter.

As discussed above, the C^1···$Si^{2,3}$ (4.1 Å) and C^1···$Si^{4,5}$ (5.1 Å) interactions between the methanol molecule bound to the silanol group and Si atoms in the SiO_2 network probably contribute to the broad interactions at 3.5−5.5 Å. However, the 4.1- and 5.1-Å peaks observed in the RDF for the capillary-condensed methanol sample at 298 K are significantly larger than those for the monolayer methanol sample (Figure 6a). In addition, the two peaks for the capillary-condensed methanol sample are gradually evolved and sharpened with decreasing temperature, in contrast with there being no significant structural change with temperature for the monolayer methanol. Thus, other additional interactions, which are sensitive to temperature, should be considered for the two peaks. It is very likely that interactions between hydrogen-bonded methanol chains also contribute to the peaks because the pore diameter (28 Å) of MCM-41 C14 corresponds to the size of about six methanol molecules if a methanol molecule has a diameter of ∼5 Å; that is, two methanol chains can be formed along the longitude of the cylindrical pores together with the monolayer methanol adsorbed on the surface. In Figure 9, a plausible model of structure for the capillary-condensed methanol is illustrated with

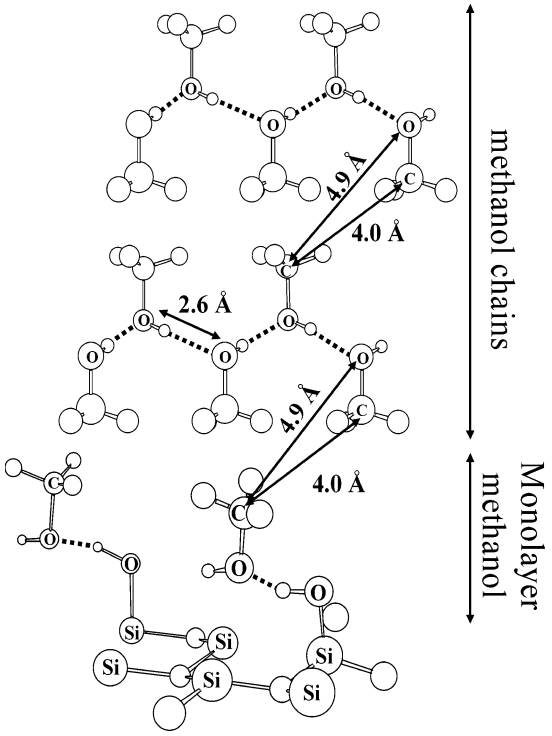

Figure 9. Structure model of capillary-condensed methanol in a pore. The dashed lines represent hydrogen bonds.

important interatomic distances. In accordance with the van der Waals radius (2.0 Å) of the methyl group, the distance of the C···C interaction between two methanol chains is estimated to be 4.0 Å and that of the C···O interaction between methyl C and hydroxyl O atoms is 4.9 Å. As seen in Figure 9, C···C and C···O interactions are present between the hydrogen-bonded methanol chains and the methanol molecules adsorbed on the surface as well. The distances of the C···C and C···O interactions are in good agreement with the 4.1- and 5.1-Å peaks, respectively. A possible reason that C···C and C···O interactions are strong in the RDF for the capillary-condensed methanol, but not significant for bulk methanol, is that the translational motions of methanol chains are strongly restricted in the MCM-41 pores, while methanol chains more loosely interact with each other in the bulk methanol because of their free three-dimensional translation motion. As seen in this model, the methanol layers may interact with each other mainly by van der Waals force, but not by hydrogen bonding. On the other hand, the previous investigation showed that the hydrogen-bonded network of water is evolved even in the MCM-41 pores.[11] This difference between methanol and water confined in the MCM-41 pores may be caused by fewer hydrogen-bonding sites and the bulkiness of methanol molecules.

As seen in Figure 7a, when the temperature is lowered, the 2.6-Å peak of O···O hydrogen bonds is gradually sharpened, suggesting that hydrogen bonds between methanol molecules are gradually ordered with temperature. The C···C and C···O interactions at 4.1 and 5.1 Å are also intensified with decreasing temperature. These findings reveal that the motions of methanol molecules in the pores are gradually restricted with decreasing temperature.

Figure 7b shows the RDFs for the capillary-condensed methanol in the smaller MCM-41 C10 pores (21 Å) at various temperatures. The RDF for the MCM-41 C10 sample at 298 K is comparable with that for the MCM-41 C14 sample.

It should be mentioned that the 4.1- and 5.1-Å peaks in the RDF for the C10 sample are larger and sharper than those for the C14 one. This feature becomes more significant with decreasing temperature. In accordance with the adsorption isotherms of methanol for the C10 and C14 pores (Figures 1 and 2), the amounts of methanol for the capillary-condensed C10 and C14 samples, which were prepared at the methanol vapor pressures of 10.0 and 12.0 kPa, respectively, are not very different from each other. However, the C10 sample has $^3/_4$ the pore diameter and $^1/_2$ the pore volume of those for the C14 sample, respectively (Table 1). Hence, methanol molecules in the C10 sample would be more closely packed than those in the C14 one. This is the reason for the larger and sharper C···C and C···O interactions between methanol layers in the C10 pores relative to those in the C14 pores. With decreasing temperature, the C···C and C···O interactions are more restricted in the C10 pores than in the C14 pores, leading to the 4.1- and 5.1-Å peaks for the C10 sample being far sharper than those for the C14 sample. The present findings are in good agreement with those on the dynamics of organic solvents confined in silica glasses by Jonas and co-workers; that is, the smaller the pore size, the more significantly the reorientational motion of organic solvents in pores is retarded with decreasing temperature.[12,13]

Least-Squares Refinements for the Structure Functions. To make a quantitative analysis on intermolecular interactions for both bulk methanol and methanol confined in the MCM-41 pores, a least-squares fitting procedure with eqs 6 and 7 in ref 11 was performed on the structure functions over the *s* range from 0.1 to 14.4 Å. In the present analysis, the intramolecular structure parameters within a methanol molecule previously determined by LANS experiments were employed.[28]

For bulk methanol at 298 K, the structure parameters have already been determined in the previous study.[15] Thus, the quantitative analysis on the structure function for bulk methanol at 298 K obtained from the present experiments was made again to confirm the previous results. In the analysis for methanol at 298 K, the structure parameters determined in the previous investigation were applied as model parameters. On the other hand, for methanol at 223−273 K, first, plausible model parameters were built up in the *r* space in a trial-and-error manner based on the structure parameters for methanol at 298 K. Consequently, the most plausible model parameters could be obtained by modifying only the numbers and temperature factors of the structure parameters for methanol at 298 K. Then, the least-squares fitting procedure was performed on the structure functions by using the structure model parameters obtained in the *r* space.

The optimized structure parameters are summarized in Table S1 in the Supporting Information. Figures 2 and 5 show that the theoretical *si*(*s*) and RDFs, which were calculated by using all of the optimized values, reproduce the observed values well, except for the ranges of $s \leq 3.5$ Å^{-1} and $r \geq 6$ Å, to which the long-range interactions not taken into account in the present analysis contribute. The distance (2.777 ± 0.004 Å) and number (1.78 ± 0.04) of O···O hydrogen bonds for methanol at 298 K are in good agreement with those (2.771 ± 0.004 Å and 1.73 ± 0.03, respectively) determined in the previous investigation[15] within the experimental errors. Figures 10 and 11 show the temperature dependencies of the distance and number of O···O hydrogen bonds for bulk methanol, respectively. As seen in Figure 10, with a decrease in temperature, the distance of O···O hydrogen bonds for bulk methanol gradually decreases to 2.720 ± 0.004 Å at 223 K. On the other hand, Figure 11 shows that the number of O···O hydrogen bonds for bulk methanol slightly increases to 1.87 ± 0.04 at 223 K. These results reveal that hydrogen-bonded methanol chains in the bulk are gradually ordered with decreasing temperature.

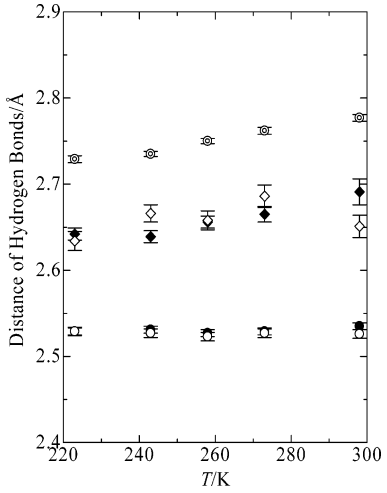

Figure 10. Distances of O···O hydrogen bonds for bulk methanol (circle within a circle), monolayer methanol in MCM-41 C14 (●) and C10 (○), and capillary-condensed methanol in C14 (♦) and C10 (◊) as a function of temperature, together with the standard deviation of σ as error bars.

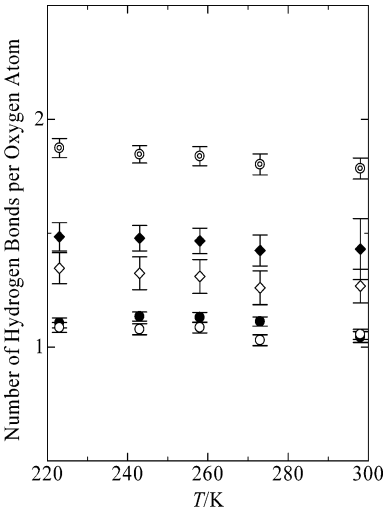

Figure 11. Numbers of O···O hydrogen bonds for bulk methanol, monolayer methanol in MCM-41 C14 and C10, and capillary-condensed methanol in both pores as a function of temperature, together with the standard deviation of σ as error bars. The symbols are the same as those in Figure 10.

For the monolayer methanol in the MCM-41 C14 and C10 pores, first, the parameters of the adsorption structure model (Figure 8) were tested to determine how they reproduced the observed RDFs. The structure model could satisfactorily explain the observed RDFs for both C14 and C10 samples at all of the temperatures investigated. Thus, a least-squares fitting was carried out on the structure functions by using the structure parameters of the adsorption structure model. In the Supporting Information, all of the optimized structure parameters for the monolayer methanol in the C14 and C10 pores were listed in Tables S2 and S3, respectively. As seen in Figures 3 and 6, the agreements between the experimental and theoretical values of *si*(*s*) and RDFs calculated by using the optimized parameter values are good, except for the long-range interactions in the ranges of $s \leq 3$ Å^{-1} and $r \geq 5.5$ Å, respectively, which are not taken into account in the present analysis.

In Figures 10 and 11, the distances and numbers of O···O hydrogen bonds for the monolayer methanol in the pores are depicted as a function of temperature. The distances of the O···O hydrogen bonds between the methanol molecule and the silanol group for the monolayer methanol in the C14 and C10 samples at 298 K were estimated to be 2.535 ± 0.004 and 2.526 ± 0.005 Å, respectively. These distances are much shorter than those of the O···O hydrogen bonds between methanol molecules in bulk methanol but comparable with that (2.56 ± 0.02 Å) for monolayer water in MCM-41 C14 pores.[11] It is thus suggested that methanol molecules adsorbed on the SiO_2 surface are influenced by the acidity of the silanol group as well as water molecules because of the large electrostatic attraction of the silanol group.[11] The numbers (1.04 ± 0.02 and 1.06 ± 0.02, respectively) of O···O hydrogen bonds between the methanol molecule and the silanol group for the C14 and C10 samples at 298 K are very close to unity, suggesting that one methanol molecule is bound mainly to one silanol group. With decreasing temperature, both the distances and numbers of hydrogen bonds for the monolayer methanol C14 and C10 samples do not significantly change. It is thus concluded that methanol molecules are strongly bound to the silanol groups on the pore surface, resulting in O···O hydrogen bonds that are less sensitive to the pore size and temperature.

As discussed in the section of total RDFs, there are two structures for the capillary-condensed methanol of the C14 and C10 samples (Figure 9): the methanol bound to the surface and the hydrogen-bonded chains of methanol molecules at the central part of pores. Thus, a structure model was built up by a combination of the adsorption structure for the monolayer methanol on the surface and the hydrogen-bonded chain structure. Additionally, nonbonding interactions between methanol layers, such as C···C and C···O interactions, were considered, as discussed above. Because the adsorption structure of methanol observed for the monolayer methanol samples should still be kept in the capillary-condensed methanol samples, the structure parameters determined for the monolayer methanol samples were employed in the model for the capillary-condensed methanol. On the other hand, it is difficult to build up a structure model of the hydrogen-bonded chain of methanol formed in the pores. Hence, the parameters of the methanol chain structure determined for bulk methanol were applied to the model parameters for the capillary-condensed methanol. The distances of the C···C and C···O interlayer interactions were assumed to be 4.0 and 4.9 Å, respectively. A model-fitting procedure using these parameters was made in the *r* space. The most plausible model parameters could be built up by modifying the numbers and temperature factors of the three structures. Then, the structure-model parameters obtained in the *r* space were optimized by using a least-squares refinement procedure on the structure functions. The optimized structure parameters for the capillary-condensed methanol C14 and C10 samples are summarized in Tables S4 and S5, respectively, in the Supporting Information. As seen in Figures 4 and 7, the observed and theoretical *si*(*s*) and RDFs calculated by using all of the optimized parameter values are in good agreement with each other, except for the ranges of $s \leq 3.5$ Å^{-1} and $r \geq 5.5$ Å, where the long-range interactions were not taken into account.

Figure 10 shows the plots of the distances of O···O hydrogen bonds for the capillary-condensed methanol in the pores as a function of temperature. The distances (2.691 ± 0.015 and 2.651 ± 0.015 Å, respectively) of O···O hydrogen bonds for the capillary-condensed methanol C14 and C10 samples at 298 K are comparable with each other but longer than those (2.535 ± 0.004 and 2.526 ± 0.005 Å, respectively) for the monolayer methanol C14 and C10 samples. Here, it should be kept in mind that both interactions of methanol−silanol on the surface and methanol−methanol at the central part of the pores contribute to the parameters of the O···O hydrogen bonds estimated for the capillary-condensed methanol samples. It is thus very likely that the hydrogen bonds of methanol−methanol at the central part are longer than those of methanol−silanol on the surface. However, the distance of the hydrogen bonds of methanol−methanol will be shorter than that for bulk methanol because the two hydrogen bonds of methanol−silanol and methanol−methanol are not observed as individual peaks in the RDFs. Thus, the O···O hydrogen bonds for methanol chains in the MCM-41 pores will be distorted from the regular ones in the bulk, as observed for hydrogen bonds among water molecules in the pores.[11] Figure 10 shows that the distances of O···O hydrogen bonds for the capillary-condensed methanol in both pore sizes decrease when the temperature decreases. However, the pore-size effect on the distance of O···O hydrogen bonds is not significant over the whole temperature range investigated.

Figure 11 shows the temperature dependence of the numbers of O···O hydrogen bonds for the capillary-condensed methanol in the pores. The number (1.43 ± 0.13) of O···O hydrogen bonds for the capillary-condensed methanol in the C14 pores at 298 K is significantly reduced from that for bulk methanol. This result also suggests that hydrogen-bonded chains of methanol at the central part of the C14 pores are distorted or partly disrupted because of the confinement effect. For the capillary-condensed methanol in the C10 pores at 298 K, the number of O···O hydrogen bonds further decreases to 1.27 ± 0.07. With decreasing temperature, however, the numbers of O···O hydrogen bonds in both pore sizes seem to increase, suggesting a slight enhancement of the methanol chains in the pores. The number of O···O hydrogen bonds in the C10 pores is not larger than that in the C14 pores over the temperature range investigated. This suggests that methanol chains in the smaller pores are more distorted than those in the larger pores.

The present results suggest that the chain structure of methanol in the MCM-41 pores is gradually ordered when the temperature decreases. However, the change in the number of O···O hydrogen bonds for the capillary-condensed methanol is less sensitive to temperature than that for water in the pores; the number of O···O hydrogen bonds among water molecules significantly increases from 2.9 ± 0.1 at 298 K to 3.4 ± 0.1 at 248 K for the capillary-condensed water confined in MCM-41 C14 pores.[11] Two factors can be responsible for the behavior of methanol confined in the pores. One of the factors is that the temperature range investigated is higher than the freezing point of methanol (175 K), while the previous experiments on water in the pores were carried out from the ambient temperature (298 K) down to supercooling temperatures (below 273 K). The other is due to the larger molecular size and fewer hydrogen-bonding sites of a methanol molecule relative to water. Hence, methanol molecules in the pores cannot easily reorient themselves to evolve their hydrogen-bonded chains with decreasing temperature. The latter is probably the main reason for the less-sensitive structure of methanol in the pores to temperature.

Conclusions

The present LAXS investigation on methanol confined in the MCM-41 C14 (diameter of 28 Å) and C10 (21 Å) pores has shown that the structure of methanol consists of the monolayer methanol on the surface and the hydrogen-bonded chains of methanol molecules at the central part of the pores. On the

MCM-41 surface, methanol molecules are strongly bound to the silanol groups with very short O···O hydrogen bonds of ~2.5 Å, as shown in monolayer water in the same pores. Thus, the structure of methanol on the surface is hardly affected by the pore size and temperature. On the other hand, the results on the capillary-condensed methanol in the MCM-41 pores have shown that the number (1.43 ± 0.13) of O···O hydrogen bonds in the 28-Å pores at 298 K is remarkably smaller than that (1.78 ± 0.04) for bulk methanol. In the 21-Å pores, the number of O···O hydrogen bonds further decreases to 1.27 ± 0.07. It is thus concluded that the O···O hydrogen bonds between methanol molecules in the pores are distorted or partly disrupted and that the distortion is more progressed in the smaller pores; that is, the pore-size effect on the methanol structure is obviously present for the capillary-condensed methanol. When the temperature is lowered, the methanol chains are gradually ordered in the pores. However, the enhancement of methanol chains in the pores with decreasing temperature is less significant than that of water. This is probably because methanol layers, such as the monolayer methanol on the surface and the methanol chains at the central part of the pores, interact with each other mainly by the van der Waals force among the methyl groups, but not by hydrogen bonding. In other words, the methanol structure cannot be three-dimensionally evolved in the pores with decreasing temperature.

Acknowledgment. This work was supported partly by grants-in-aid [Grants 12640500, 15550016 (T.T.), and 15076211 (T.Y.)] from the Ministry of Education, Culture, Sports, Science, and Technology, Japan.

Supporting Information Available: All of the optimized structure parameters obtained from the present LAXS experiments (Tables S1−S5) are available free of charge via the Internet at http://pubs.acs.org.

References and Notes

(1) Clark, J. W.; Hall, P. G.; Pidduck, A. J.; Wright, C. J. *J. Chem. Soc., Faraday Trans. 1* **1985**, *81*, 2067.

(2) Steytler, D. C.; Dore, J. C.; Wright, C. J. *Mol. Phys.* **1983**, *48*, 1031.

(3) Dore, J. C.; Dunn, M.; Chieux, P. *J. Phys. Coll. C1* **1987**, *48* (Suppl. 3), 457.

(4) Bellissent-Funel, M.-C.; Lal, J.; Bosio, L. *J. Chem. Phys.* **1993**, *98*, 4246.

(5) Bellissent-Funel, M.-C.; Bradley, K. F.; Chen, S. H.; Lal, J.; Teixeira, J. *Physica A* **1993**, *201*, 277.

(6) Bellissent-Funel, M.-C.; Chen, S. H.; Zanotti, J.-M. *Phys. Rev. E: Stat. Phys., Plasmas, Fluids, Relat. Interdiscip. Top.* **1995**, *51*, 4558.

(7) Hansen, E. W.; Stöcker, M.; Schmidt, R. *J. Phys. Chem.* **1996**, *100*, 2195.

(8) Morishige, K.; Nobuoka, K. *J. Chem. Phys.* **1997**, *107*, 6965.

(9) Takamuku, T.; Yamagami, M.; Wakita, H.; Masuda, Y.; Yamaguchi, T. *J. Phys. Chem. B* **1997**, *101*, 5730.

(10) Takahara, S.; Nakano, M.; Kittaka, S.; Kuroda, Y.; Mori, T.; Hamano, H.; Yamaguchi, T. *J. Phys. Chem. B* **1999**, *103*, 5814.

(11) Smirnov, P.; Yamaguchi, T.; Kittaka, S.; Takahara, S.; Kuroda, Y. *J. Phys. Chem. B* **2000**, *104*, 5498.

(12) Liu, G.; Li, Y.; Jonas, J. *J. Chem. Phys.* **1991**, *95*, 6892.

(13) Ballard, L.; Jonas, J. *Langmuir* **1996**, *12*, 2798.

(14) Morishige, K.; Kawano, K. *J. Chem. Phys.* **2000**, *112*, 11023.

(15) Takamuku, T.; Yamaguchi, T.; Asato, M.; Matsumoto, M.; Nishi, N. *Z. Naturforsch., A: Phys. Sci.* **2000**, *55a*, 513.

(16) (a) Yamaguchi, T.; Hidaka, K.; Soper, A. K. *Mol. Phys.* **1999**, *96*, 1159. (b) Yamaguchi, T.; Hidaka, K.; Soper, A. K. *Mol. Phys.* **1999**, *97*, 603.

(17) Narten, A. H.; Levy, H. A. *J. Chem. Phys.* **1971**, *55*, 2263.

(18) Narten, A. H. *J. Chem. Phys.* **1972**, *56*, 5681.

(19) Beck, J. S.; Vartulli, J. C.; Roth, W. J.; Leonowicz, M. E.; Kresger, C. T.; Schmitt, K. D.; Chu, C. T.-W.; Olson, D. H.; Sheppard, E. W.; McCullen, S. B.; Higgins, J. B.; Schlenker, J. L. *J. Am. Chem. Soc.* **1992**, *114*, 10933.

(20) Dollimore, D.; Heal, G. G. R. *J. Appl. Chem.* **1964**, *14*, 119.

(21) Yamanaka, K.; Yamaguchi, T.; Wakita, H. *J. Chem. Phys.* **1994**, *101*, 9830.

(22) (a) Ihara, M.; Yamaguchi, T.; Wakita, H.; Matsumoto, T. *Adv. X-Ray Chem. Anal., Jpn.* **1994**, *25*, 49. (b) Yamaguchi, T.; Wakita, H.; Yamanaka, K. *Fukuoka Univ. Sci. Rep.* **1999**, *29*, 127.

(23) Furukawa, K. *Rep. Prog. Phys.* **1962**, *25*, 395.

(24) Krogh-Moe, J. *Acta Crystallogr.* **1956**, *2*, 951.

(25) Norman, N. *Acta Crystallogr.* **1957**, *10*, 370.

(26) Johanson, G.; Sandström, M. *Chem. Scr.* **1973**, *4*, 195.

(27) Yamaguchi, T. Doctoral Thesis, Tokyo Institute of Technology, Tokyo, Japan, 1978.

(28) Tanaka, Y.; Ohtomo, N.; Arakawa, K. *Bull. Chem. Soc. Jpn.* **1984**, *57*, 644.